

ADVANCES IN NUMERICAL MODELLING OF CRASH DUMMIES

Ruud Verhoeve, Robert Kant

TNO Automotive
The Netherlands

Laurent Margerie

TNO Automotive
France

Paper Number 152

ABSTRACT

Nowadays virtual testing and prototyping are generally accepted methods in crash safety research and design studies. Validated numerical crash dummy models are necessary tools in these methods. Computer models need to be robust, accurate and CPU efficient, where the balance between accuracy and efficiency is depending on the nature of the study performed.

This paper presents the application of advanced multibody-modelling techniques, in order to generate crash dummy models that are accurate as well as CPU efficient. Two techniques, deformable body modelling and arbitrary surface modelling, are combined. Their application is presented by means of an example model: the Hybrid III 50th percentile thorax. The method for generating the model is explained, after which the accuracy and efficiency of the model is illustrated by presenting some simulation results.

INTRODUCTION

To support the automotive industry with their passive safety research and design studies, numerical simulation tools are needed and used at an ever-increasing level. Virtual prototyping and testing have become generally accepted. Numerical simulations with realistic and accurate models, such as multibody and finite element models, allow a highly significant reduction of both time and costs over working with hardware prototypes only. In the process of crash safety design optimisation, numerous parameters play a role, which has resulted in an increasing need for extensive and detailed parameter sensitivity studies. For this reason there is also an increasing need for

numerical models that are both accurate in terms of response and efficient in terms of CPU costs.

In general, three important desired features can be identified for numerical models in virtual design studies: (1) little time and effort needed to generate them, (2) a high level of accuracy in predicting reality, and (3) little CPU time needed for the simulations. Mainly depending on the phase of the vehicle design process in which the model is used, the priority of these three aspects varies. The early phases of the design process generally ask for many simulations with relatively simple models and limited requirements on accuracy. In the later phases the complexity of the models and the demands on the accuracy increase and the number of simulations decreases.

In the field of crash safety R&D, the most widely used numerical modelling techniques are finite element (FE) modelling and multibody (MB) modelling [1,2]. Of these two techniques, FE modelling is generally the most detailed and therefore it is also expected to provide a higher level of accuracy. Nevertheless, the accuracy is often limited because of problems such as limitations in the mesh refinement (due to the necessary CPU efficiency), in the element formulations, and in the applied material models. FE models are generally not very efficient in terms of CPU costs, what makes them less suitable for sensitivity and optimisation studies. Multibody models are usually much more efficient with respect to CPU costs, making them better suitable as tools for extensive design optimisation studies. Due to their simplified nature, their responses are often expected to be less accurate at detailed level. Therefore their range of application is often more directly determined by their range of validation.

Following the need for fast and accurate computer modelling in crash safety engineering, crash dummy models also need to be both accurate and CPU efficient. The aspect of limited modelling effort is considered less relevant. Modelling efforts may be high, since the model needs to be generated only once, after which it can serve as a tool in many different numerical research and design studies.

This paper describes the application of two more advanced multibody-modelling techniques in a crash dummy component model developed for MADYMO [5]. These techniques enable multibody crash dummy models to become more realistic in geometry as well as in mechanical behaviour, while keeping high CPU efficiency with respect to FE models. The two techniques presented are deformable body modelling and modelling with arbitrary surfaces. The attention is focussed primarily on the procedures followed for the implementation of deformable bodies and arbitrary surfaces, rather than on the model itself. The development of a 50th percentile male Hybrid III thorax model is used as an example to explain the applied modelling procedures.

DEFORMABLE BODIES

In a multibody environment deformable structures are generally modelled in a simplified way, by rigid bodies that are connected by joints and spring-damper elements. In FE models such structures are modelled in a much more detailed way, resulting in a large number of degrees of freedom. An alternative way of modelling deformable structures is by means of deformable bodies [6,7]. In a deformable body, the structural deformation is represented by a linear combination of user-defined displacement fields (deformation modes), which are prescribed in the form of coupled nodal motions. Stiffness and damping matrices describe the dynamic characteristics of the set of deformation modes in a linear way. For each deformable body, the number of degrees of freedom describing the structural deformation is limited to the number of deformation modes. The objective is to define only a few modes that together can cover the deformation patterns that occur in realistic loading conditions. With a well-chosen set of deformation modes, relatively complex deformations can be described accurately in an efficient way. Note that due to the coupling of nodal displacements, a more detailed representation with

more nodes and elements does not increase the number of degrees of freedom, keeping the model CPU efficient. For this reason, modelling with deformable bodies is very attractive for developing dummy models with high demands on both accuracy and CPU efficiency [8,13].

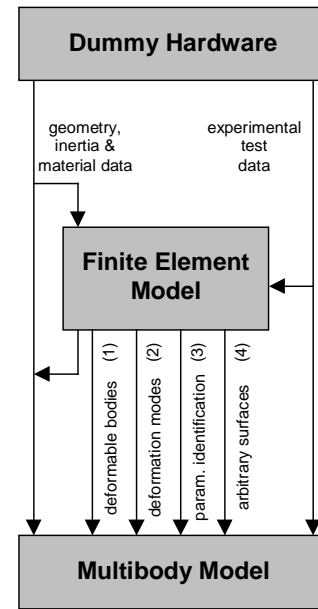


Figure 1. Procedure for the development of multibody models using deformable body and arbitrary surface technology.

In this paper, the 50th percentile male Hybrid III thorax is used as an example to explain the procedure of implementing deformable bodies [11,12]. For the Hybrid III thorax it can be expected that explicit modelling of rib deformation will contribute to an accurate prediction of sternum deflection and viscous criterion. Although the Hybrid III thorax can show large deformations, its deformation pattern in frontal loading conditions is relatively predictable. Furthermore, quasi-static ribcage loading tests indicated that the rib stiffness is reasonably linear, also for larger deformations. Therefore the Hybrid III thorax promises to be quite suitable for being modelled by means of deformable bodies. Figure 1 illustrates the procedure applied for modelling dummy components with deformable bodies. Although the FE thorax model is an important tool in this procedure, the explanation below will focus only on the development of the multibody model with the deformable bodies.

Hardware and multibody model design

The Hybrid III 50th percentile male thorax basically consists of a spine box and a sternum connected by 12 ribs (see figure 2). Being left-right symmetric, they form six rib pairs that are each shaped differently. Each rib is made of a curved steel plate, with damping material at the inner side of each half rib. The sternum consists of two metal plates that have a plastic sheet connected in between. This plastic sheet, the so-called bib, connects the sternum to the ribs and to the upper end of the spine box. At each side of the sternum, the bib and the front ends of the ribs are interconnected with two aluminium stiffener strips. Rubber rib stop bumpers restrict compression of the sternum. A foam pad (covering frontal thorax only) and a rubber jacket cover the thorax.

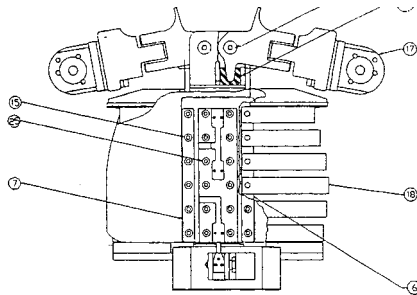


Figure 2. The Hybrid III thorax: hardware.

In the multibody model, twelve deformable bodies are used to model each rib together with its overlying jacket section. Rigid bodies represent the spinebox, sternum and left and right stiffener strips and their connection to the deformable body ribs can be modelled with kinematic joints and dynamic restraint models. The mass of the thorax and jacket is distributed realistically over the rigid bodies and deformable body nodes. Arbitrary surfaces are used to represent the geometry of the thorax and the jacket (see next section). Figure 3 shows the multibody thorax model.

Implementation of deformable bodies and modes

Implementation of the deformable bodies is relatively straightforward: the rib and jacket nodal positions in undeformed state can be derived directly from the mesh of a FE thorax model (figure 1, step 1). After the deformable rib bodies have been implemented,

for each rib a set of sensible deformation modes needs to be determined and implemented (figure 1, step 2). Here again the FE thorax model is used. Simulation of realistic loading conditions provided thorax deformation output that helped in determining a suitable set of deformation modes.

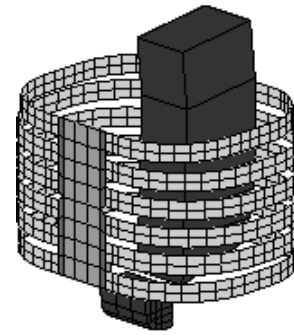


Figure 3. The Hybrid III thorax: multibody model.

In the ribcage deformation output four main patterns could be distinguished, which need to be modelled to reproduce ribcage deformations accurately. The corresponding rib deformation patterns are referred to as 'frontal blunt rib bending', 'frontal local rib bending', 'lateral rib bending' and 'vertical rib bending'. The blunt and local frontal rib bending patterns represent responses due to two extreme cases of frontal compression. These two patterns can be translated to two different deformation modes for each rib. Combinations of these two modes can approximate ribcage responses to intermediate cases of frontal compression. 'Lateral rib bending' occurs when the sternum is moving in lateral direction with respect to the spinebox. Two deformation modes need to be defined to describe both left and right 'lateral ribcage shearing'. In combination with the frontal modes, these lateral modes can also reproduce intermediate, oblique ribcage loading cases. 'Vertical rib bending' occurs when the sternum is moving in vertical direction with respect to the spinebox. A fifth rib deformation mode could be defined for this, but rotational joints connecting the ribs to spinebox are believed to represent vertical ribcage deformation more efficiently and with sufficient accuracy. The remaining four rib deformation modes are illustrated in figure 4.

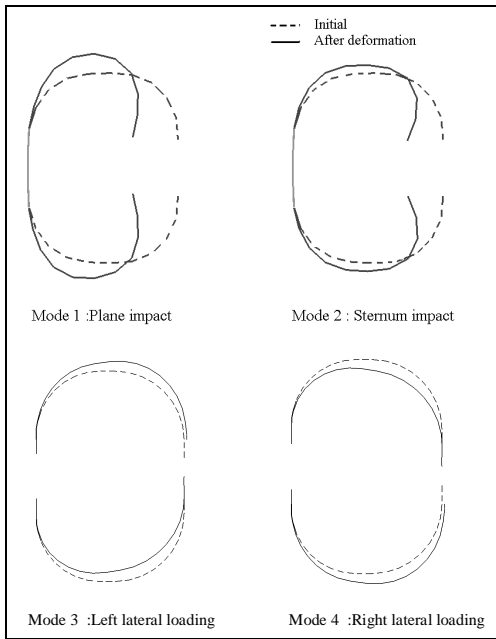


Figure 4. The four rib deformation modes in the multibody thorax model.

To implement the four deformation modes for the twelve ribs, again the FE thorax model could be used. Three different loading cases were simulated with the FE model:

- frontal ribcage loading (plate),
- frontal sternum loading (vertical cylinder),
- directly applied lateral sternum loading,

Each deformation mode can be derived from the deformed state nodal positions output of the FE simulations. For each rib these nodal positions form one deformation mode relative to the undeformed rib nodes. By mirroring the output, the left and right lateral modes could be derived from one lateral loading case.

Identification of stiffness and damping parameters

After defining and implementing the deformation modes, the components of stiffness and damping matrices need to be identified (figure 1, step 3). The diagonal terms describe the stiffness and damping of each mode separately. The cross terms enable coupling of the different deformation modes. The parameters can be identified by again using the FE thorax model and/or experimental test data.

For identification of the diagonal terms of the stiffness and damping matrices, the loading cases that

were used to determine the modes were simulated both quasi-static and dynamic. With quasi-static simulations the rib stiffness values for each mode were determined. The dynamic loading simulations, with several velocities, enables identification of the corresponding damping values. The cross-terms can be determined based on loading cases that form different combinations of two of the loading cases above.

When all parameters have been identified, simulating a set of realistic impact tests can validate the multibody model. In case the correlation between tests and simulations is not satisfactory, actions should be taken to improve the model. Analysis of the differences found can indicate whether only the stiffness and damping characteristics need to be re-calibrated or extra deformation modes are needed to improve the model.

ARBITRARY CONTACT SURFACES

External loads on a dummy are mostly transferred through soft material layers that represent human flesh, skin or clothing. The compliance of the outer dummy surface varies, depending on the material and thickness of those soft layers and on the supporting structures underneath. Traditional multibody algorithms represent this compliance by contact definitions between analytical surfaces like ellipsoids, planes and cylinders, using a penetration based contact algorithm. To enable a more accurate description of this load transfer, both the geometry and the compliance of the outer surface of the dummy can be modelled in more detail.

In order to model the geometry more accurately, arbitrary surfaces can be used. Arbitrary surfaces are modelled as meshes of contact elements, of which all nodes are supported to rigid bodies or deformable bodies (see former section). Although FE meshes are used to describe the surfaces, no FE solver is used for calculating surface deformation. Deformation of arbitrary surfaces can occur only due to relative motion of different supporting bodies and/or deformation of supporting deformable bodies.

Load transfer via the arbitrary surfaces can be modelled by definition of contact interactions. An advanced, penetration based contact algorithm was developed for arbitrary surfaces in MADYMO [5].

The advantage over the traditional algorithm used for analytical surfaces is that it uses stress functions instead of force functions. This introduces sensitivity to the shape of the contacting objects (e.g. focal versus blunt impact).

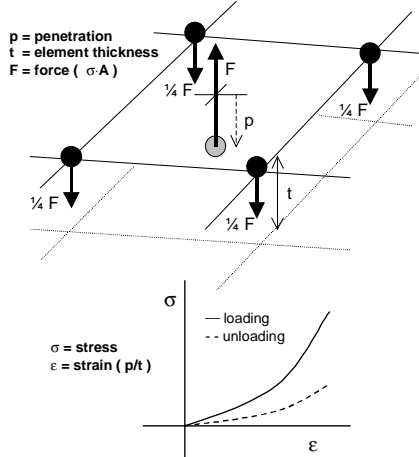


Figure 5. Contact algorithm for arbitrary surfaces.

With the advanced contact algorithm, contacts can be defined with other arbitrary surfaces, but also with analytical and finite element surfaces. The compliance of the dummy's soft materials is taken into account by allowing penetrations in the contacted arbitrary surfaces (see figure 5). For each penetrating node the local contact stress will be determined based on the user-defined stiffness characteristics for that surface. The contact force is obtained by multiplying the contact stress by the area around the node, which is the average of the adjacent element areas. This force is transferred from the arbitrary surface to the supporting rigid or deformable body. For the element penetrated by the node, the same contact stress is transferred to forces on the connecting nodes.

The contact stiffness characteristics of an arbitrary surface is defined in the form of stress-strain functions for loading and, in case of hysteresis being included, for unloading (see figure 5). The strain is defined here as the ratio of penetration and element thickness. On crash dummy components, the compliance generally varies over the outer surface due to variations in the thickness and the mechanical properties of the soft material layer. The element thickness distribution over the surface can be based directly on the thickness of the real soft material

layer. Where the mechanical properties vary significantly, different stress-strain functions can be used. Besides stiffness functions also damping characteristics can be defined to model rate effects. This method of contact definition assumes that compression stiffness dominates the load transfer, multiple material layers may be lumped together non-deforming structures support the soft outer materials. Where these assumptions become invalid, the element thickness and/or the stiffness functions can be modified to correct for this.

To illustrate the principle of contact definitions between arbitrary surfaces, a simple test was simulated with a finite element and a multibody model. In this test a rigid sphere penetrated a low-density, soft block by means of a prescribed motion. The test set-up is illustrated in figure 6.

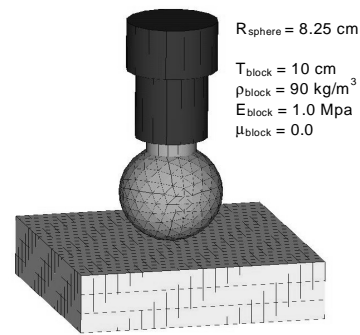


Figure 6. Rigid sphere penetrating soft deformable block: simulation set-up.

In the FE model the rigid sphere was modelled with shell elements and the deformable block was modelled with hexahedral elements and linear elastic isotropic material behaviour. In the multibody model sphere and block were represented by arbitrary surfaces. To model the compliance of the block, a contact function was derived from the block material parameters. Assuming one-dimensional block deformation due to the penetrating sphere (only compression is taken into account), a stress-strain contact function could be derived from the material properties. The contact function is defined by multiplying the Young's modulus with the logarithmic strain for the block (for large deformations). Equation 1 shows the stress-strain definition.

$$\sigma(p/T_{\text{block}}) = -E_{\text{block}} \cdot \ln(1-(p/T_{\text{block}})) \quad (1.)$$

The linear strain is defined as the ratio of the block penetration and the block thickness. Compression stresses are defined as positive.

With both models 10 ms simulations have been performed with a simulation time step of 1.0 μ s. No contact damping and friction were defined in the models. The reaction force on and the displacement of the sphere were obtained as output signals. These signals were used to derive the reaction force vs. penetration curves for both simulations. The results are shown in figure 7.

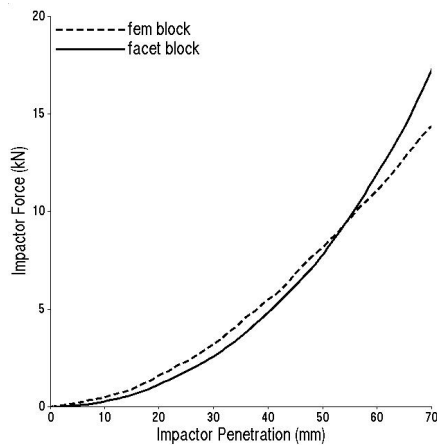


Figure 7. Rigid sphere penetrating soft deformable block: reaction force on sphere vs. penetration in block.

The differences seen can be explained by the three dimensional deformation effects that are not incorporated in the multibody model. In spite of these differences, the signals are corresponding quite well. Only for penetrations of more than 60 mm the differences become more significant. This indicates that without taking 3D deformation effects into account, contact interactions can be modelled quite realistically with arbitrary surfaces. To illustrate the CPU efficiency of the multibody model, it should be noted that the multibody simulation cost about half a minute of CPU time, where the FE model cost more than six minutes. Both simulations were run on a SGI Octane workstation with a single 300 MHz R12k processor.

For the multibody thorax model introduced in the previous section, arbitrary surfaces were applied for the ribs, spinebox, sternum and the jacket. These surfaces could again be derived from the FE thorax

model (figure 1, step 4). For the ribs and jacket the surfaces were directly attached to the deformable body nodes. In this way these surfaces deform realistically along with thorax deformations. The central frontal and back regions of the jacket surface were attached to respectively the rigid sternum and spinebox bodies, and the upper region was attached to the rigid shoulder bodies. Figure 8 shows the jacket surface regions supported to the different bodies.

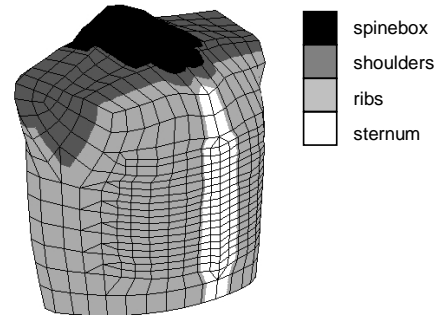


Figure 8. Jacket surface: supported to different bodies.

To avoid nodes getting stuck behind the jacket surface the arm and neck and lower openings are closed. A single stress-penetration function was used for the whole jacket surface. The surface compliance varies due to the varying surface thickness, which is shown in figure 9.

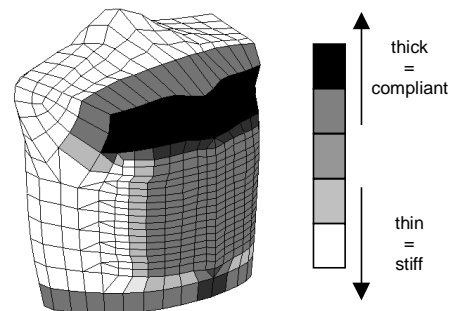


Figure 9. Jacket surface: varying surface thickness.

PERFORMANCE OF THE NEW THORAX MODEL

For the development and validation of the model a series of more than 30 thorax component tests were used, in which impact type and severity were varied.

The tests included both blunt thorax impacts and local impacts on several locations on the sternum and ribs. To illustrate the performance of the newly developed thorax model, two simulated experiments are presented. Figure 10 shows the set-up of a thorax component test. In this example a supported thorax is hit frontally with a square flat rigid plate, having an impact speed of 6.0 m/s. The chest deflection signals of test and simulation show good correlation, as can be seen in figure 11. It can be seen that particularly the loading phase and the peak level are reproduced quite well. To run this 80 ms MADYMO simulation, just a little more than 1 minute of CPU time was needed on a SGI Octane workstation with a single 300 MHz R12k processor.

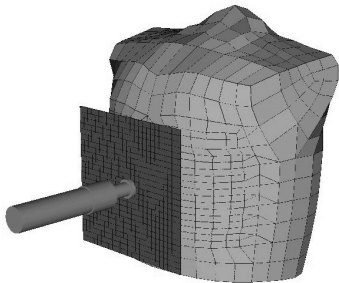


Figure 10. Hybrid III thorax component test: frontal plate impact, simulation set-up.

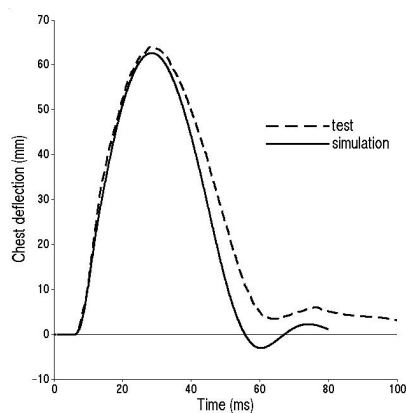


Figure 11. Hybrid III thorax component test: frontal plate impact, chest deflection vs. time.

The new multibody thorax model has been incorporated in a complete multibody dummy model, in which all other dummy components were also modelled using arbitrary surfaces. This complete Hybrid III 50th percentile male dummy model was used for simulation of a sled test. The set-up of test

and simulation is shown in figure 12. A belted Hybrid III dummy was seated in a rigid seat that was fixed directly onto the sled. The feet were placed on a rigid footrest. The sled was decelerated from 50 to 0 km/h with a maximum deceleration of 21g.

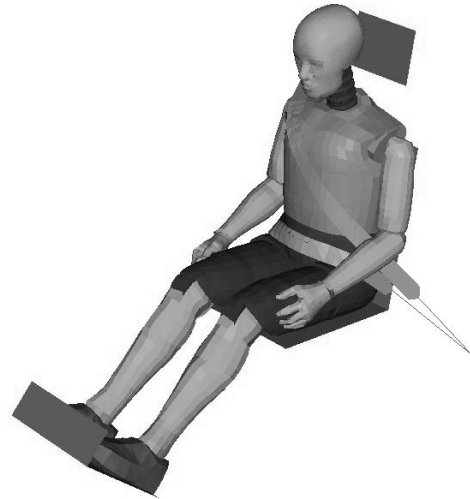


Figure 12. Sled test with belted 50th percentile Hybrid III dummy: simulation set-up.

In the simulation the seat planes were modelled with single element arbitrary surfaces. A FE belt model was used to enable an accurate representation of the dummy-belt interactions [14]. The sled test was simulated in MADYMO with a runtime of 200 ms. Comparison of test and simulation results for the chest deflections shows adequate correlation of the signals, as can be seen in figure 13. The simulation took just over 20 minutes CPU time on a SGI Octane workstation with a single 300 MHz R12k processor.

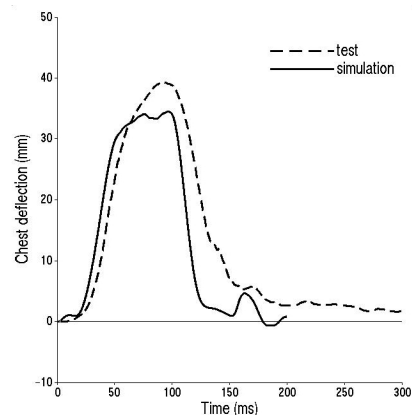


Figure 13. Sled test with belted 50th percentile Hybrid III dummy: chest deflection vs. time.

DISCUSSION & CONCLUSION

Procedures were presented for application of two multibody techniques in crash dummy models. These techniques were deformable body modelling and arbitrary surface modelling. The modelling procedures were explained by means of an example model, the Hybrid III 50th percentile thorax. The two techniques allow multibody models to become more accurate in both geometric representation and prediction of mechanical behaviour. The application of deformable bodies has proved to enable a realistic and accurate representation of complex structural deformations with a limited number of degrees of freedom. Modelling with arbitrary instead of analytical surfaces enables a more realistic geometric representation that, together with the advanced contact algorithm, proved to enable more realistic modelling of contact load transfer in multibody models.

Both multibody-modelling techniques were also found to be efficient in terms of CPU costs. It has to be noted though, that the CPU efficiency of complete numerical models depends not only on the dummy model, but also on how its environment is modelled. When for example a CPU efficient dummy model is placed in a very detailed full vehicle FE model, the overall gain in efficiency will be limited. Nevertheless, dummy models that are both fast and accurate are very valuable for performing large parameter sensitivity or design optimisation studies by means of virtual testing. Studies on the effects of stochastic variations in restraint systems and/or vehicles are a good example here, since such studies are expected to become more important in future crash safety R&D.

The CPU efficiency of multibody dummy models is not only advantageous for the users. For the model developer it provides the possibility of using larger test matrices for simulations in the development process, so that the models can be validated for a more extensive range of loading conditions. Apart from their efficiency, multibody models have the advantage to be more robust than FE models in terms of stability. Also the multibody thorax model presented in this was found to be very robust.

As was illustrated with the thorax model, both advanced modelling techniques discussed here proved to be very valuable tools for developing crash dummy models that are both robust, accurate and fast.

ACKNOWLEDGMENTS

The authors express their thanks to Ford Dearborn for providing experimental test data.

REFERENCES

1. Rao S.S. (1982). The Finite Element method in engineering. Pergamon Press, Oxford.
2. Shabana A.A. (1989). Dynamics of multibody systems. Wiley-Interscience.
3. Philippens M., Nieboer J.J., Wismans J. (1991). An advanced database of the 50th percentile Hybrid III dummy (SAE-910813).
4. Lasry D., Schlosser L., Marcault P., Rentschler S. LeRenard A., Haug E. (1994). Finite element dummies for frontal impact. paper 94S1W20.
5. TNO Automotive (1999). MADYMO Theory Manual and User's Manual 3D, version 5.4.
6. Shabana A.A. (1989). Transient analysis of flexible multi-body systems, Part I: Dynamics of flexible bodies. Comp. Meth. in Applied Mechanics and Eng., vol 54 pp.75-91.
7. Koppens W.P. (1988). The dynamics of Deformable Bodies, TU Eindhoven PhD thesis, Eindhoven University of Technology.
8. Koppens W.P., Lupker H.A., Rademaker C.W. (1993). Comparison of modeling techniques for flexible dummy parts. STAPP Conference 1993, SAE933116.
9. Fountain M., Happee R., Wismans J., Lupker H., Koppens W. (1996). Hybrid modelling of crash dummies for numerical simulation. IRCOBI conference, 1996.
10. Fountain M.A., Koppens W.P., Lupker H.A. (1996). Flexible body modelling in MADYMO. Presented at the 6th International MADYMO Users' meeting. April 1-2, 1996, Amsterdam, the Netherlands.
11. User's Manual for the 50th percentile Male Hybrid III Dummy (1998 edition).
12. Happee R., Kant A.R., Abramowski E., Feustel J. (1998). The load path from upper legs to chest in the Hybrid III dummy; Experiments and

simulations. ESV Conference 1998, Paper 98-S9-W-24.

13. Van der Made R. Margerie L., Hovenga E., Kant R., Co J., Xu B., Sriram N.S., Laituri T. (2001). Development of a Hybrid III 5th percentile Facet Dummy Model. SAE paper 2001-01-1050.
14. Fraterman E., Lupker H.A. (1993). Evaluation of belt modelling techniques. SAE930635.